J. Membrane Biol. 12, 247–272 (1973)

An Analysis of the Relationship between the Current and Potential Generated by a Quantum of Acetylcholine in Muscle Fibers without Transverse Tubules

Peter W. Gage and Robert N. McBurney

School of Physiology and Pharmacology, University of New South Wales, Kensington, N.S.W., Australia

Received 4 December 1972

Summary. Miniature end plate potentials (MEPPs) were recorded in glycerol-treated muscle fibers with four microelectrodes which were used to determine the passive electrical characteristics of the same fibers. Voltage responses which were computed from miniature end plate currents (MEPCs) and the passive cable properties of a fiber, agreed very closely with experimentally recorded MEPPs confirming the hypothesis that MEPPs spread passively along a muscle fiber. The model was used to analyze the effect of variations in synaptic current and the properties of a muscle fiber on the post-synaptic response. The decrement of MEPPs was exponential for distances up to 1 to 2 mm from an origin but then deviated from the initial exponential. Variations in the growth time of the input current up to 1 msec had little effect on computed MEPPs whereas an increase in the decay time constant caused a significant increase in MEPP amplitude and effective "space constant." An increase in the internal resistivity of a muscle fiber increased MEPP amplitude at the origin but decreased the effective space constant. The amplitude of MEPPs was inversely proportional to the 1.5 power of the "diameter" of a muscle fiber, and the MEPP space constant increased as the square root of the diameter. The amplitude of MEPPs is not necessarily determined by the "input" resistance of the muscle fiber. Changes in input resistance caused by changes in membrane resistance would have little effect on the amplitude or decrement of MEPPs.

At chemical synapses, neurotransmitters are released from presynaptic terminals in discrete multimolecular quanta. At the neuromuscular junction each of these quanta of transmitter generates an inward current, the miniature end plate current (MEPC), across the subsynaptic membrane of the muscle fiber. This current depolarizes the muscle membrane giving a miniature end plate potential (MEPP). During neuromuscular transmission, an end plate potential is produced by the summation of the effects of many of these quanta.

The aims of this investigation were twofold; first, to test the hypothesis that the spread of the postsynaptic potential is a purely passive process

and second, to evaluate the influence of the time course of the current and the characteristics of the postsynaptic cell on the time course, amplitude and decrement of postsynaptic potentials. MEPPs were studied because the MEPC can be reasonably well defined (Gage & Armstrong, 1968; Gage & McBurney, 1972). Muscles were glycerol-treated to decouple the transverse tubules from the surface (Eisenberg & Gage, 1967; Howell & Jenden, 1967; Eisenberg & Eisenberg, 1968; Gage & Eisenberg, 1969; Howell, 1969) and hence to simplify the equivalent circuit (Fig. 1) and the mathematical model.

The neuromuscular junction offers an ideal situation for constructing and testing a model of synaptic transmission. The time course, amplitude and origin of the MEPC have been determined using voltage-clamp techniques (Gage & Armstrong, 1968; Gage & McBurney, 1972) and the electrical characteristics and synaptic responses of the postsynaptic cell can be recorded in a structure of observable geometry. Such complete information would be difficult, if not impossible, to obtain at any other synapse. The results obtained here with detubulated muscle fibers should be applicable, at least qualitatively, to unmyelinated nerve fibers.

By using an equation giving the voltage response to an impulse of current in a cable with the equivalent circuit of a glycerol-treated muscle fiber, and by convolution of an MEPC with the impulse response, voltage responses as a function of time and distance along the cable are obtained. These responses are found to agree well with experimentally recorded MEPPs and hence are consistent with the hypothesis of passive spread of MEPPs as proposed by Fatt & Katz (1951). The model has proved useful in predicting the influence of the time course of synaptic currents and membrane parameters on postsynaptic potentials. In particular, the results reveal that small changes in membrane capacitance have more influence than changes in membrane resistance on the amplitude, time course, and spread of postsynaptic potentials.

Materials and Methods

Preparation and Experimental Techniques

The preparation used was the glycerol-treated (Eisenberg & Gage, 1967; Howell & Jenden, 1967; Gage & Eisenberg, 1969; Howell, 1969) sartorius muscle of toads (*Bufo marinus*). Experiments were done in winter months. An end plate region was located by insertion of a microelectrode (10 to 20 MΩ) in a region where the motor nerve gave off fine branches. If MEPPs could be recorded, and their rise-time was less than 2 msec, three more microelectrodes were inserted in the same fiber in the same region. The first electrode was used either to pass a current pulse across the fiber membrane or to record

membrane potential. In the first instance a rectangular current pulse was passed across the membrane with the first electrode and the voltage responses at three points along the fiber were recorded with the other three electrodes. Then an MEPP was recorded with the four electrodes in the same fiber. Distances between the electrodes were measured against a graticule in the eyepiece of a Wild M5 stereomicroscope ($\times 100$).

The normal toad solution contained (mmoles/liter): NaCl, 115; KCl, 2.5; $CaCl_2$, 1.8; Na phosphate buffer, 3; pH = 7.2. The frequency of MEPPs in this solution was very low (less than 1 per sec) and it was difficult to record them on fast oscilloscope sweeps. The frequency was increased by raising the NaCl concentration to 175 mmoles/liter. The MEPCs which are used in computations here, were recorded in the same hypertonic solution (Gage & McBurney, 1972).

Theory

If a glycerol-treated muscle fiber is regarded as an infinite cable ($x = -\infty \rightarrow +\infty$), with a unit circuit as shown in Fig. 1*B*, the partial differential equation (Hodgkin & Rushton, 1946) which describes the relationship between voltage (V), distance (x) and time (t), is

$$\frac{1}{r_i}\frac{\partial^2 V(x,t)}{\partial x^2} - c_m\frac{\partial V(x,t)}{\partial t} - \frac{V(x,t)}{r_m} = 0$$

where r_i is the internal resistance per unit length, r_m is the membrane resistance per unit length, and c_m is the membrane capacitance per unit length.

By using Laplace transforms with respect to time, a differential equation which describes the voltage response of this cable to an input current, $I(0, t)$, at $x = 0$ can be derived (*see*, e.g., Carslaw & Jaeger, 1963):

$$\frac{d^2\bar{V}(x,s)}{dx^2} - (Q(s))^2\bar{V}(x,s) = 0 \tag{1}$$

where s is the transform of the time variable t and $\bar{V}$ is the transformed voltage.

The coefficient $Q(s)$ depends on the equivalent circuit under consideration and in this case is given by

$$Q(s) = \sqrt{\frac{r_i}{r_m}(1+\tau_m s)} \tag{2}$$

where τ_m is the membrane time constant.

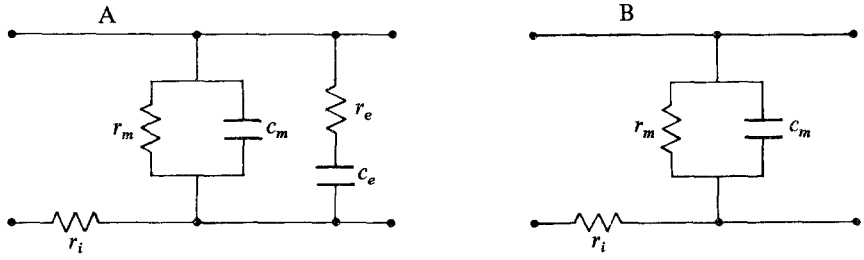

Fig. 1. Equivalent circuits of a unit length of membrane of a normal (*A*) and a glycerol-treated (*B*) muscle fiber. r_m and c_m are the resistance and capacitance of the surface membrane, r_i the internal resistance, and r_e and c_e, the resistance and capacitance of the transverse tubular system (or sarcoplasmic reticulum) per unit length of fiber

The solution of the differential equation shown in (1), using the boundary condition $\bar{V}(\pm\infty, s)=0$, is

$$\bar{V}(x, s)=\frac{\bar{I}(0, s)\, r_i}{2Q(s)}\, e^{-xQ(s)} \tag{3}$$

where $\bar{I}(0, s)$ is the transform of the input current.

A solution for real time depends on whether Eq. (3) can be inverted with the inclusion of $Q(s)$ and the appropriate function for $I(0, s)$. There are a number of methods for obtaining an inversion of Eq. (3) with a function for $I(0, t)$ which describes a miniature synaptic current. Jack and Redman (1971) have used the function $I=\alpha^2 Te^{-\alpha T}$ as a description of a synaptic current and they have obtained an analytical solution for the voltage response of a linear electrical cable.

The analytical solution of Jack and Redman (1971) is not used here because MEPCs are not well described by $\alpha^2 Te^{-\alpha T}$ under all conditions. For example, currents generated by acetylcholine in the presence of procaine (Gage & Armstrong, 1968) cannot be described by this equation.

We have obtained voltage responses by convolution of the input current $I(0, t)$ with the impulse response of the cable.

$$V(x, t)=\int_0^t I(0, u)\, G(x, t-u)\, du \tag{4}$$

where $G(x, t-u)$ is the impulse response of the cable at the time $t-u$.

$$G(x, t)=\frac{1}{2}\sqrt{\frac{r_m r_i}{\tau_m \pi t}}\, e^{\frac{-r_i \tau_m x^2}{4 r_m t}}\, e^{\frac{-t}{\tau_m}}. \tag{5}$$

[Eq. (5) is very similar to previously derived equations (Hodgkin, in Fatt & Katz, 1951; Noble & Stein, 1966; Jack & Redman, 1971).]

Because the input current does not need to be transformed, the method of convolution is very useful for synaptic currents which cannot be described by a single function, but can be described by a combination of functions.

The MEPC is described by

$$I(0, t)=\begin{cases} Pt/TG & t<TG \\ Pe^{-(t-TG)/TD} & t\geqq TG. \end{cases} \tag{6}$$

(P=peak amplitude of current, t=time from start of current flow, TG=duration of growth phase, and TD=time constant of decay phase).

A computer program, which allowed convolution of the impulse response of a cable with the equivalent circuit of a glycerol-treated muscle fiber, and an input current, was written for a PDP-8 computer (Digital Equipment) from Eq. (4).

Computation

For comparison of observed and predicted MEPPs in individual fibers the cable parameters, r_m, r_i, and τ_m, recorded for the fiber were used in the program, and the input current was defined by Eq. (6) with appropriate parameters.

Initially, TG and TD were set in the middle of the physiological range (Gage & McBurney, 1972), at 0.2 and 1.7 msec, respectively. The amplitude P was varied in the range 3.6 to 7.0 namps until the amplitude of one MEPP (usually the largest) was fitted. In this way the time course and amplitude of a voltage response at any distance x from the origin could be computed for a particular muscle fiber.

In the second section, the computer was used to test the influence of the parameters used in the program, on the voltage response. The "standard" parameters were: $r_m = 1.59 \times 10^5\ \Omega\ \text{cm}$, $r_i = 3.98 \times 10^6\ \Omega\ \text{cm}^{-1}$ and $c_m = 5.03 \times 10^{-8}\ \text{F cm}^{-1}$. Assuming a circular cross-section, and a "standard" fiber diameter of 80 μm, specific values of $R_m = 4{,}000\ \Omega\ \text{cm}^2$, $R_i = 200\ \Omega\ \text{cm}$ and $C_m = 2 \times 10^{-6}\ \text{F cm}^{-2}$ are obtained. The d-c space constant is 2 mm and the time constant τ_m is 8 msec. The standard values were based on the values found experimentally in glycerol-treated toad sartorius fibers (Table 1). In the second section the standard input current, representing an MEPC, was described by Eq. (6) with $P = 5$ namps, $TG = 0.2$ msec and $TD = 2$ msec.

Results

Comparison of Recorded and Computed MEPPs

Cable Parameters. The cable constants of glycerol-treated muscle fibers were determined from recordings of voltage responses to rectangular current pulses (Hodgkin & Rushton, 1946; Katz, 1948; Fatt & Katz, 1951; *see also* Gage & Eisenberg, 1969) with four microelectrodes in a fiber. The input resistance R_0, space constant λ, and time constant τ_m were determined conventionally from graphs. The amplitudes of the d-c voltage responses in a fiber were plotted semilogarithmically against distance from the site of current injection and a straight line drawn through the points. Extrapolation of the line to the ordinate gave V_0, the voltage response at the input and hence the input resistance R_0. The abscissal value where the voltage was $V_0 e^{-1}$ gave the space constant λ. The time constant of the membrane was determined by plotting the time for a voltage response to reach 50% of its final steady value, against distance from the site of current injection. By extrapolation of a straight line through the points, the "50% time" at the input was determined and hence the time constant (Gage & Eisenberg, 1969).

The cable parameters of nine glycerol-treated fibers in which d-c responses and MEPPs were recorded using four microelectrodes are shown in Table 1. The values of membrane resistance r_m, membrane capacitance c_m, and internal resistance r_i per centimeter length of fiber, were determined from the equations; $r_m = 2\lambda R_0$, $c_m = \tau_m / r_m$ and $r_i = 2R_0/\lambda$. By assuming an internal resistivity of 200 Ω cm (Fatt, 1964; Gage & Eisenberg, 1969; Dulhunty & Gage, 1973) the "specific" resistance R_m and capacitance C_m per square centimeter of membrane, and the "diameter" d_c of each fiber, were calculated.

The purpose of calculating "specific" membrane capacitances was to confirm that the fibers were indeed "detubulated". All nine fibers had a membrane capacitance (mean $C_m = 1.81\ \mu\text{F cm}^{-2}$; SE $= 0.18\ \mu\text{F cm}^{-2}$) sig-

Table 1. Electrical constants of glycerol-treated muscle fibers

Fiber	R_0 (MΩ)	λ (mm)	τ_m (msec)	r_m ($\times 10^5$ Ω cm)	r_i (MΩ cm^{-1})	c_m ($\times 10^{-8}$ F cm^{-1})	R_m (Ω cm^2)	C_m (μF cm^{-2})	d_c (μm
56.1	0.53	2.24	8.0	2.37	4.75	3.37	5472	1.46	73
56.3	0.79	1.75	10.2	2.77	9.05	3.68	4613	2.21	53
56.4	0.72	1.60	9.5	2.30	9.00	4.13	3850	2.47	53
57.1	0.50	1.80	7.5	1.80	5.57	4.16	3829	1.96	68
57.2	0.90	1.60	8.2	2.80	13.00	2.93	4305	1.91	48
57.3	0.39	1.92	3.8	1.50	4.10	2.53	3725	1.02	79
57.4	0.61	1.12	4.6	1.36	10.90	3.38	2075	2.22	48
57.6	0.57	1.38	5.5	1.57	8.30	3.50	2744	2.01	56
60.1	0.63	1.64	3.8	2.07	7.70	1.84	3738	1.02	58
						Mean	3817	1.81	
						SE	329	0.18	

Cable parameters and passive electrical properties of the surface membrane of nine glycerol-treated toad sartorius muscle fibers. R_0, λ and τ_m were measured from graphs. R_m, C_m and d_c were calculated by assuming an internal resistivity of 200 Ω cm.

nificantly lower than in normal fibers (4 to 8 μF cm^{-2}). As in frog sartorius muscle (Gage & Eisenberg, 1969) the mean membrane resistance of glycerol-treated toad sartorius fibers (3,817 Ω cm^2) was not significantly different from that of normal fibers. Apparent fiber diameters were measured in all fibers but were not used to calculate R_m and C_m because of the possible error introduced by assuming a circular cross-section.

Determination of the Origin of MEPPs. To compute voltage responses which could be compared with MEPPs it was necessary to determine the origin of the MEPPs. This was usually done by straddling an end plate region with the four microelectrodes and recording an MEPP simultaneously from four points in the fiber. An MEPP recorded in this way is shown in Fig. 2*A*. The number beside each trace shows the distance in microns between an electrode and the reference electrode. When the peak amplitudes of these MEPPs were plotted semilogarithmically against the distance from the reference electrode, a straight line could be drawn through three of the points (Fig. 2*B*). If a straight line is drawn through the fourth point with a gradient equal to, but the negative of, the gradient of the first line, the intercept of the two lines gives the origin of the MEPP. This method is based on the assumption, which seems reasonable, that the "space constant" for MEPPs is the same on either side of the origin. The distance from the origin x of each microelectrode was determined in this way. This graphical

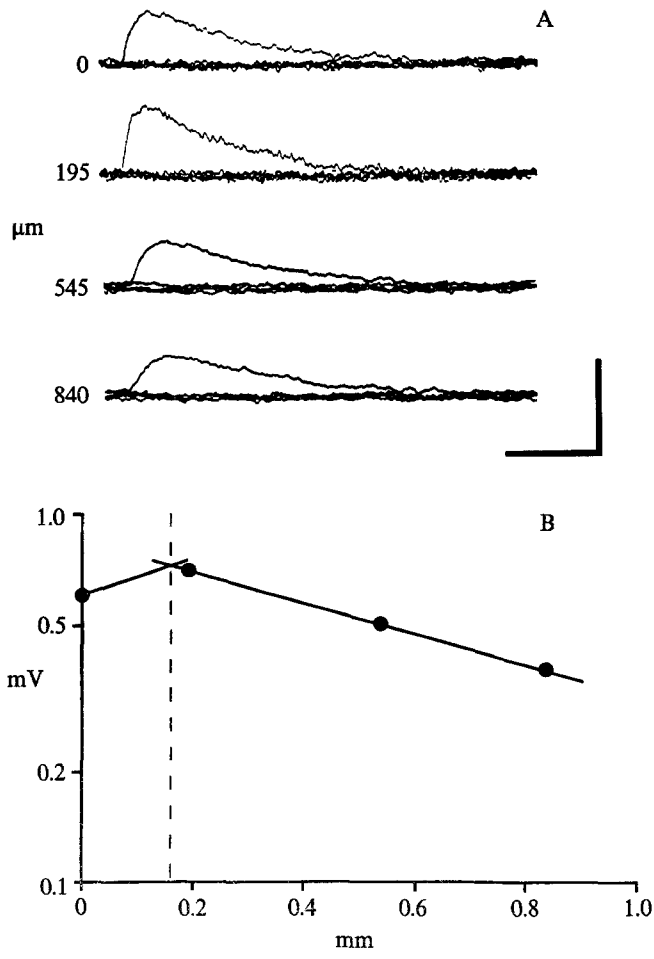

Fig. 2. (*A*) A miniature end plate potential recorded with four microelectrodes in an end plate region. The relative positions of the electrodes are shown on the left (μm). Vertical calibration, 1 mV. Horizontal calibration, 4 msec. (*B*) Semilog plot of the amplitude of a miniature end plate potential against distance from an end electrode. The intercept of the two lines gives the position of the origin (vertical broken line) and the amplitude of the miniature end plate potential at the origin

method was used also when there were two electrodes on each side of an origin.

The origin of successive MEPPs at one end plate could be detected using this method. Nineteen MEPPs were recorded in a fiber in which four microelectrodes straddled the end plate region. For any one MEPP, the amplitudes with the four microelectrodes were plotted semilogarithmically against the distance from the first electrode and straight lines were drawn through the first and second, and the third and fourth points. The intercept

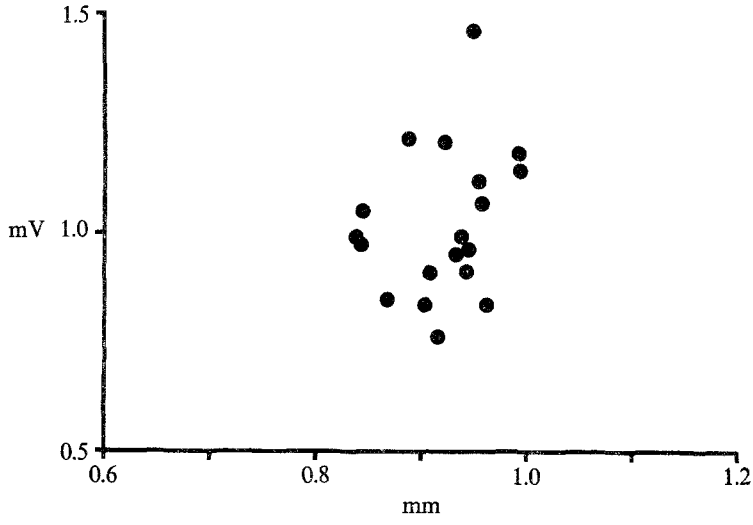

Fig. 3. The origins of miniature end plate potentials recorded with four microelectrodes straddling an end plate. The origin was determined graphically as in Fig. 2*A* and Fig. 4*A*. *Ordinate:* amplitude of potentials at the origin. *Abscissa:* distance from an end electrode

of each of these sets of two lines is shown as a point on the graph in Fig. 3. The points show the original amplitude and the origin of each of the nineteen MEPPs. In this fiber, the physiological end plate determined in this way was at least 180 μm in length and, at any origin, the amplitude of an MEPP could vary widely. Although the magnitude of the gradients of the two lines through one set of MEPPs was not significantly different, the gradients did vary during successive MEPPs reflecting the variation in the decay time of MEPCs (Gage & McBurney, 1972).

Computed MEPPs. When MEPPs had been recorded in a fiber, and r_m, r_i, τ_m and the distances of the electrodes from the origin had been determined, the cable parameters were inserted in the impulse function for convolution by computer with the MEPC (*see* Materials and Methods). A computed MEPP was obtained for each value of x corresponding to the distance of an electrode from the origin of the MEPP. When the appropriate MEPC amplitude had been found, the four computer-predicted potentials for each of the four different distances were generally found to agree very closely with the MEPPs recorded experimentally.

As has been shown (Gage & McBurney, 1972), the decay time of MEPCs varies in any one fiber and from fiber to fiber. Although using the average value of 1.7 msec as a standard decay time of MEPCs gave reasonable fits to observed MEPPs in all nine fibers, it was found that perfect fits could

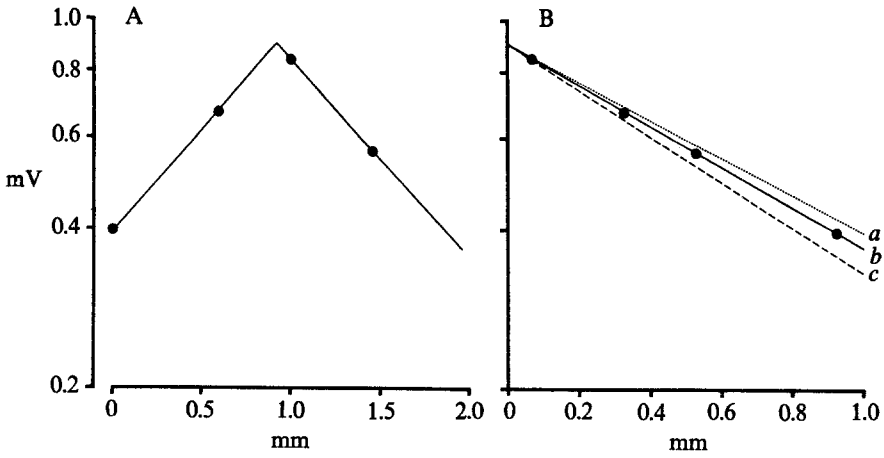

Fig. 4. (*A*) Location of the origin. A semilog graph of the amplitude of a miniature end plate potential against distance from an end electrode (mm). The intercept of the two lines gives the origin, hence the distance of each of the four electrodes from the origin. (*B*) The same four potentials plotted against distance from the origin, the position of which was determined in *A*. The straight line *b* through the four points was computed for an input current with a time constant of decay of 1.7 msec. The lines *a* and *c* show the computed decrement of potential for input currents with time constants of decay of 2.5 and 1 msec, respectively

sometimes be obtained by varying the decay time within the physiological range of 1.5 to 2 msec (*see* Fig. 8, Gage & McBurney, 1972).

The usual procedure is illustrated in Fig. 4. In this fiber, MEPPs and responses to rectangular current pulses were recorded at a resting membrane potential of −63 mV. The amplitude of MEPPs was plotted semilogarithmically against distance from the first electrode and two straight lines were drawn through each set of two points to determine the origin (Fig. 4*A*). The points were then plotted semilogarithmically against distance from the origin in Fig. 4*B*. The slope of a line through the four points was best fitted by using an MEPC with a decay time of 1.7 msec with the fiber parameters in the computer program. The amplitude of the MEPC which shifted the computed line onto the points (Fig. 4*B*) was 6.5 namps. It was always necessary to select a current amplitude by trial and error because of the large variation which is found (Gage & McBurney, 1972) but the selected value invariably fell in the physiological range, usually above the modal value because of the tendency to select for comparison large MEPPs to improve the signal-to-noise ratio. The amplitude of an MEPC acts purely as a scaling factor and does not affect the decrement or time course of MEPPs. A rise-time of 0.2 msec always provided a very good fit, perhaps because MEPPs are rather insensitive to this parameter (*see later*). In this

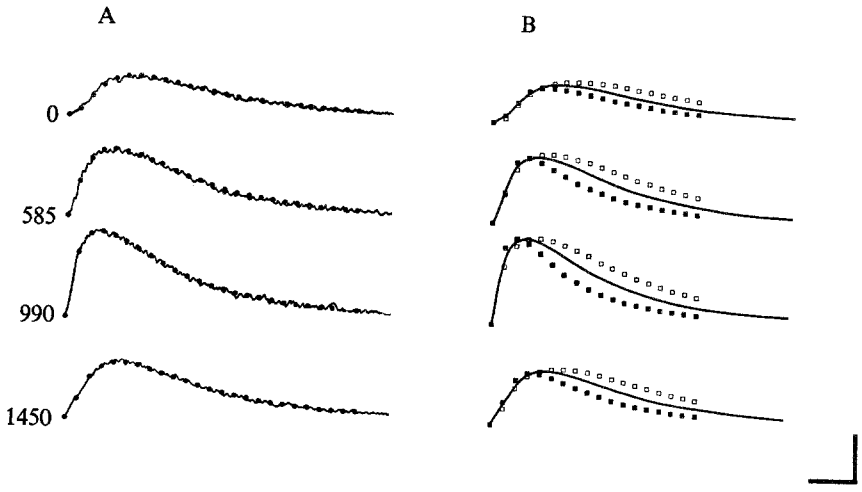

Fig. 5. (*A*) Records of a miniature end plate potential obtained with four microelectrodes at the distances shown on the left (μm) from an end microelectrode. Computed miniature end plate potentials are shown as superimposed points (decay time constant = 1.7 msec). (*B*) Miniature end plate potentials computed for the fiber in *A*, in response to input currents with decay time constants of 2.5 msec (open squares) and 1 msec (filled squares). Smoothed traces of the same miniature end plate potentials as in *A* are shown for comparison (lines)

fiber (Fig. 4), the voltage response to an input current with an amplitude of 6.5 namps and a decay time of 1.7 msec fitted the points very well (Fig. 4*B*, *b*). The other two lines, *a* and *c*, were computed from currents with decay times of 2.5 and 1.0 msec, respectively, and are included to show the sensitivity of the method.

A comparison of recorded MEPPs and voltage responses to the input current with a decay time of 1.7 msec (filled circles) is shown in Fig. 5*A*. The predicted voltage responses for the two other decay times can be seen in Fig. 5*B* (1.0 msec, filled squares; 2.5 msec, open squares) compared with a smooth curve traced from the recorded MEPPs.

Another example of a comparison between computed and observed MEPPs in a fiber with a membrane potential of −55 mV is shown in Fig. 6. The measured cable parameters for this fiber were $r_m = 2.8 \times 10^5\ \Omega\ \text{cm}$, $r_i = 1.3 \times 10^7\ \Omega\ \text{cm}^{-1}$, and $\tau_m = 8.2$ msec. The current input (MEPC) had an amplitude of 4.6 namps and a decay time of 1.8 msec. The correspondence between the recorded MEPPs and computed responses (filled circles) argues strongly for the hypothesis of a passive spread of MEPPs.

In one experiment, the microelectrodes did not straddle the origin of MEPPs but it was still possible to determine the origin and to compare predicted and observed potentials. The four MEPPs were plotted semi-

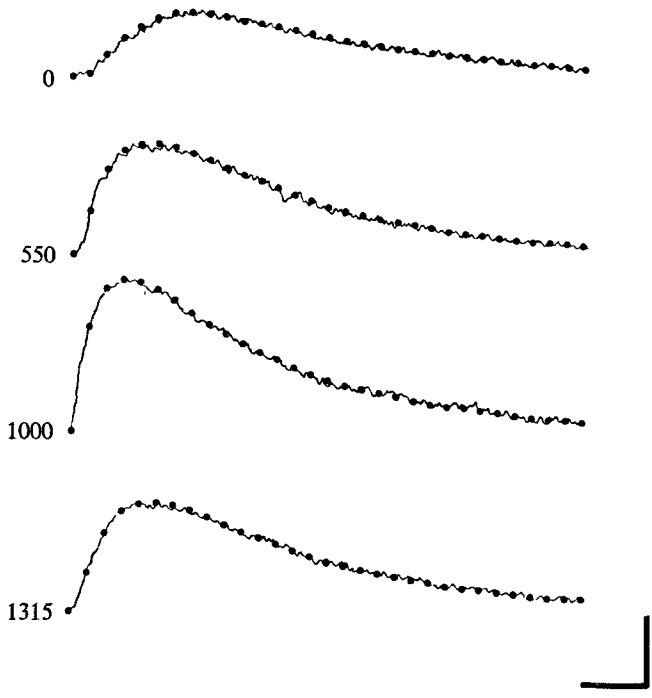

Fig. 6. A miniature end plate potential recorded at the distances shown on the left (μm) from an end electrode. Superimposed are points showing computed voltage responses at each distance, for an input current decaying with a time constant of 1.8 msec. Vertical calibration, 0.5 mV. Horizontal calibration, 2 msec

logarithmically against distance (from the first electrode) and a straight line drawn through the points. The slope of this line could be fitted uniquely by one decay time of an MEPC, which was 1.3 msec. Using this decay time, a growth time of 0.2 msec, and a variable current amplitude, MEPPs were computed for a series of distances from the origin. These were superimposed on the largest of the four recorded MEPPs until the distance x and the current amplitude which gave a good fit were obtained. The amplitude of current which gave a good fit in this fiber was 5.2 namps but this variable was a scaling factor only and had no effect on the time course which was, in contrast, very sensitive to x. The distance of the other MEPPs from the origin was calculated from the electrode separations, and these distances, with the MEPC, were used in the computer to predict the amplitude and time course of the three other MEPPs. This method again gave a good fit between predicted and observed MEPPs.

The consistent and repeated agreement between predicted and observed voltage responses to an MEPC confirms the hypothesis that a quantum

of transmitter produces in a muscle fiber a localized source of current which spreads along a passive cable. The computer program which had been developed to test this hypothesis proved very useful for evaluating quantitatively the influence of various parameters on MEPPs.

Factors Affecting MEPPs

The current generated by a quantum of transmitter is neither rectangular nor sinusoidal in shape (Gage & Armstrong, 1968; Gage & McBurney, 1972). There is, therefore, no direct way (Hodgkin & Rushton, 1946; Eisenberg & Johnson, 1970) of predicting the exact influence of the structure or electrical properties of a muscle fiber on the voltage response generated by an MEPC. The methods described above were used to evaluate the influence of the resistance of the membrane and sarcoplasm, the capacitance of the membrane, and fiber size on MEPPs. The effect of the time course of the synaptic current on the voltage response has been determined also.

In the analyses which follow, the standard muscle fiber has the following parameters: diameter = 80 μm; $r_m = 1.59 \times 10^5$ Ω cm; $r_i = 3.98 \times 10^6$ Ω cm^{-1}; $\tau_m = 8$ msec. These give the specific parameters: $R_m = 4{,}000$ Ω cm^2; $R_i =$ 200 Ω cm; $C_m = 2 \times 10^{-6}$ F cm^{-2} which correspond approximately to the mean values obtained experimentally.

The standard MEPC was represented by Eq. (6), with $P = 5$ namps, $TG = 0.2$ msec, $TD = 2$ msec.

Decrement of MEPPs. A current with the time course of an MEPC was used to compute voltage responses in a standard muscle fiber.

The amplitudes of MEPPs (Fig. 7*A*) were plotted on a logarithmic ordinate against the distance from the current source (Fig. 7*B*, filled circles). At distances up to 1 mm, the relationship between amplitude and distance x is essentially exponential (broken line) but the points deviate from the exponential at distances greater than 1 to 2 mm (Fig. 7*B*). Convolution of a rectangular current pulse (50 msec long) with the impulse response gave the relationship between the amplitude of the response and distance, shown in Fig. 7*B* (solid line). It is clear that at distances up to 10 mm at least, the decrement of the maximum voltage response to a constant current is less than the decrement of the computed response to an MEPC. A straight line (broken line) can be drawn through the points from 0 to 1 mm (Fig. 7*B*). The fall in the amplitude of MEPPs recorded up to 2 mm from an origin was generally found to be reasonably exponential and there was good agreement between the computed and actual decrement of MEPPs. In the following analyses, the MEPP space constant was measured

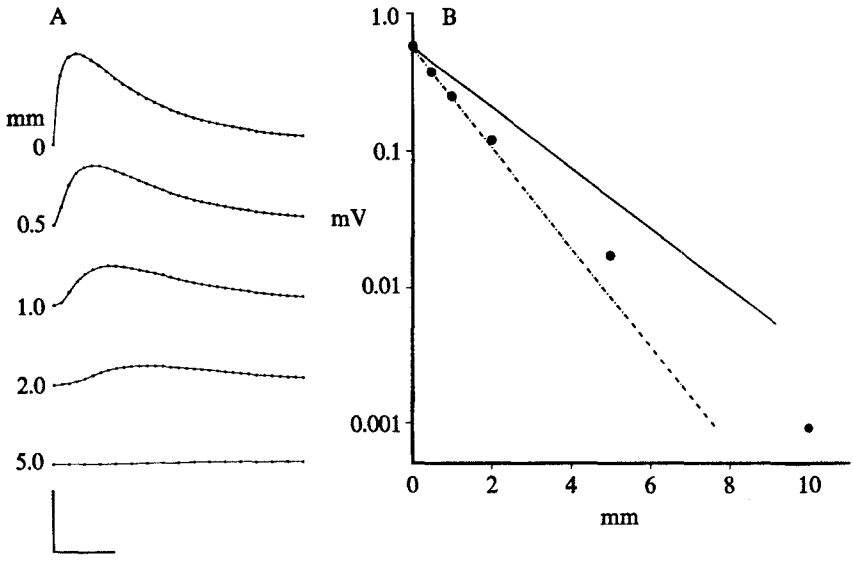

Fig. 7. (*A*) Miniature end plate potentials computed for five distances (shown on the left in millimeters) from a point of injection of a standard current ($P=5$ namps, $TG=$ 0.2 msec, $TD=2$ msec) into a cable with the electrical properties of the standard, glycerol-treated muscle fiber. Vertical calibration, 0.4 mV. Horizontal calibration, 4 msec. (*B*) A semilogarithmic plot of the amplitude of the computed voltage responses shown in *A* against distance from the current input (filled circles). The broken line is drawn through the points at 0, 0.5 and 1 mm. The solid line shows the decrement of a d-c response computed for this fiber

from a line drawn through the peak height of the voltage responses at distances up to 1 mm from the origin.

An exponential decay of the amplitude of MEPPs would be expected if the voltage response at the origin were sinusoidal (Eisenberg & Johnson, 1970). The space constant which can be measured from the line in Fig. 7*B* would be obtained with a sinusoidal voltage of approximately 25 Hz. However, the voltage response is not sinusoidal at the origin and therefore it is hardly surprising that the peak height of MEPPs deviates from the initial exponential further from the origin. The important point is that the d-c space constant is no measure of the decrement of MEPPs: with normal MEPCs, the MEPP space constant must be less than the d-c space constant.

Influence of the Time course of the Current. An MEPC is a brief displacement of charge across a small part of the subsynaptic membrane, and this generates capacitative and ionic currents across neighboring membrane. The voltage response obviously depends on the time course of the current, and resistive and capacitative properties of the fiber. These relationships are now explored quantitatively.

Growth-Time of Synaptic Current. The growth time *TG* of the input current, in the range observed for MEPCs (Gage & McBurney, 1972), has relatively little influence on computed MEPPs. The voltage responses at the origin ($x=0$) for four standard currents with different *TG*'s (Fig. 8*A*, inset) are shown in Fig. 8*A*. Other parameters in the program were standard. The peak height of MEPPs was plotted against *TG* in Fig. 8*B*. This lack of sensitivity of an MEPP to growth time of the MEPC is fortunate because the first phase of an MEPC is very rapid (Gage & Armstrong, 1968; Gage & McBurney, 1972) and therefore difficult to record. Any small error in determining *TG* in the range 0.2 to 1 msec would have little effect on the

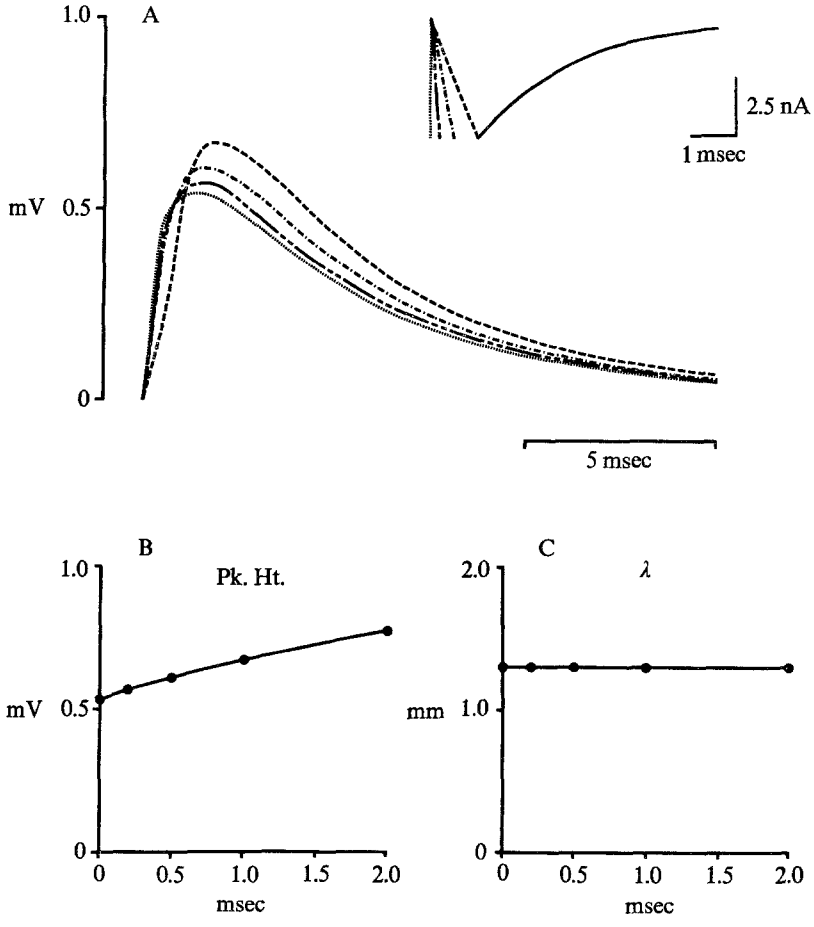

Fig. 8. (*A*) Voltage responses at the origin computed for standard input currents (inset) with varying growth times (0, 0.2, 0.5 and 1 msec). Calibrations for inset, 2.5 namps and 1 msec. Large horizontal calibration, 5 msec. (*B*) Relationship between peak height of computed responses and growth time of the current input. (*C*) Effect of growth time of the current on the space constant λ of the computed potentials

computed potentials. With a growth time of 0.2 msec, the peak of an MEPP occurred at approximately 1.5 msec and its amplitude was 0.57 mV. When a growth time of 0.5 msec was used (one of the longer *TG*'s found experimentally), the peak of the MEPP occurred at much the same time and was 0.61 mV in amplitude. As can be seen in Fig. 8*C*, in which the MEPP space constant was plotted against *TG*, the growth time of the current in this range had essentially no effect on the decrement of MEPPs.

Decay-Time of Synaptic Current. The changes in the rise-time of the current have very little effect on the amount of charge crossing the membrane at the origin and would not be expected to have a significant effect on the voltage response.

In contrast, the time constant of decay *TD* of the synaptic current, which has a much greater effect on the charge displaced across the membrane, had a marked influence on the amplitude and time course of MEPPs (Fig. 9). When the time constant was increased from 0.5 to 10 msec the peak height increased threefold. Even from 1 to 5 msec, the peak height was approximately doubled (from 0.43 to 0.81 mV) by the increase in *TD*. This relationship between MEPP amplitude and *TD* is illustrated graphically in Fig. 9*B*. As the decay time increases, the amplitude of the MEPP increases towards the maximum (2 mV) given by a rectangular current input of amplitude $P=5$ namps. It can be seen that the relationship is very steep in the physiological range (1 to 4 msec).

The MEPP space constant is also very sensitive to *TD*, again especially in the physiological range (Fig. 9*C*). When *TD* was increased from 1 to 5 msec, the MEPP space constant increased from 1.02 to 1.6 mm. As *TD* was increased further, the MEPP space constant approached the d-c space constant (2 mm).

Influence of the Electrical Properties of the Postsynaptic Cell. If the voltage response at the origin were sinusoidal, with a frequency of 25 Hz, the membrane resistance of 4 KΩ cm^2 would be in parallel with an impedance (contributed by the capacitance of 2 μF/cm^2) of 3.2 KΩ cm^2, giving a total impedance of approximately 1.8 KΩ cm^2. Doubling the membrane resistance to 8 KΩ cm^2 would increase the total impedance by only 28% to 2.3 KΩ cm^2. This would increase the input impedance of the standard fiber, and hence the amplitude of an MEPP at the origin by 13%. It is clear that as the membrane resistance increases, it will have progressively less effect on MEPP amplitude. The assumption of a sinusoidal input has been used to illustrate that membrane resistance might be expected to have relatively little effect on MEPPs. The influence of membrane

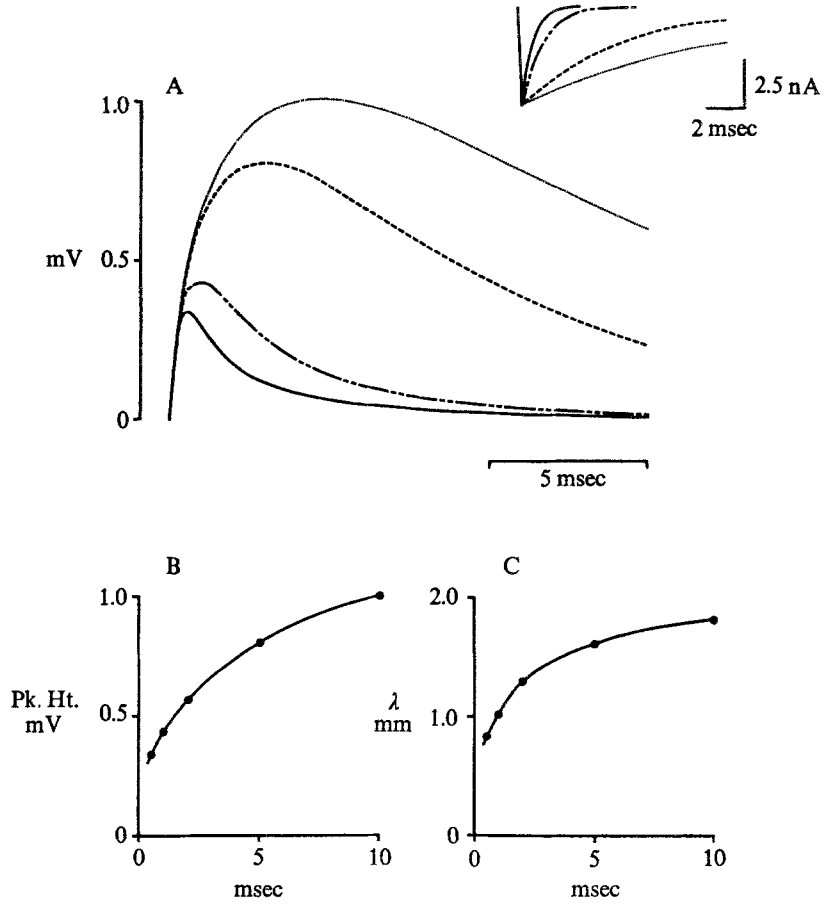

Fig. 9. (*A*) Voltage responses at the origin computed for standard input currents (inset) with varying decay time constants (0.5, 1, 5 and 10 msec). Calibrations for inset, 2.5 namps and 2 msec. Long horizontal calibration, 5 msec. (*B*) Relationship between peak height of computed responses and the time constant of decay of the current. (*C*) Relationship between the space constant of the responses and the time constant of decay of the current

resistance on MEPPs was examined analytically using the methods described before.

Membrane Resistance. Although the membrane resistance used in computations was the membrane resistance per unit length r_m, results are expressed here in terms of "specific" membrane resistance R_m, which is a more general parameter, independent of fiber diameter and proportional to r_m. In Fig. 10*A* are shown computed MEPPs at the origin in a standard fiber with a membrane resistance of 500, 2,500, 6,500 and 10,500 $\Omega\,\text{cm}^2$. As membrane resistance increased, the amplitude and time to peak of MEPPs increased, but not remarkably over this rather wide range. In fact,

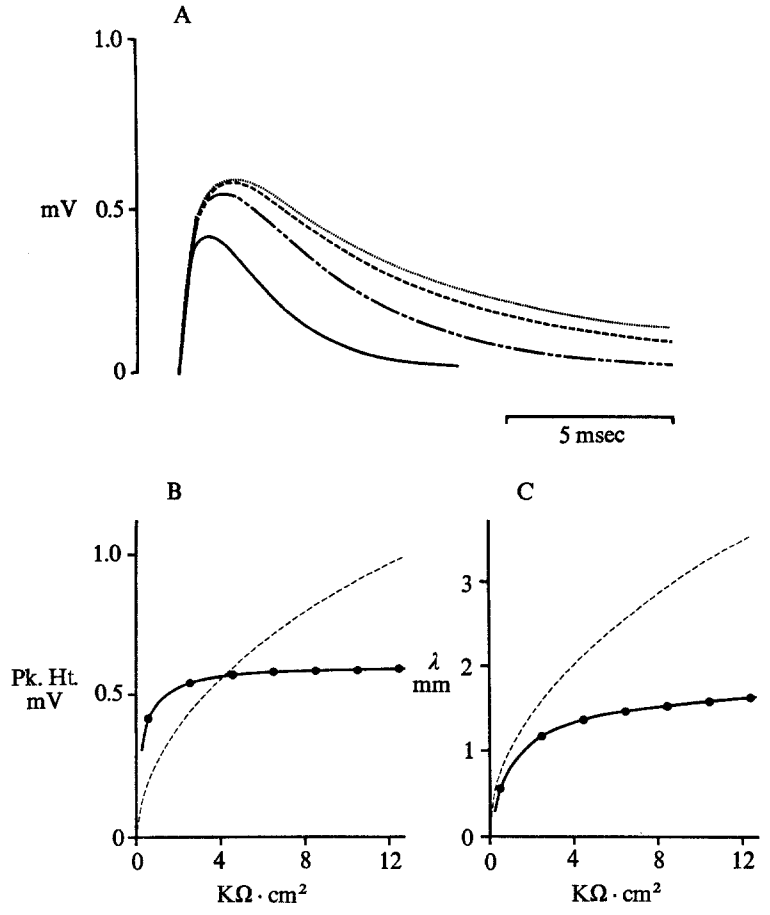

Fig. 10. (*A*) Miniature end plate potentials computed from the standard current in the standard fiber with variations in membrane resistance (from above down: 10,500, 6,500, 2,500 and 500 Ω cm²). Horizontal calibration, 5 msec. (*B*) Relationship between peak height of computed potentials and membrane resistance (KΩ). The broken line shows the relationship for a rectangular current input (1.4 namps). (*C*) Relationship between the space constant and membrane resistance with the standard input current (points and solid line). The broken line shows the relationship for a rectangular current input

the amplitude of MEPPs only increased from 0.42 to 0.59 mV as R_m increased 20-fold. The effect is illustrated graphically in Fig. 10*B* and it can be seen that membrane resistance affected the MEPP amplitude significantly only below 3,000 Ω cm² which is approximately the normal value in these fibers. The broken line in Fig. 10*B* illustrates for comparison the effect of membrane resistance on the amplitude of the voltage responses to a rectangular current input (1.4 namps).

Membrane resistance affects the MEPP space constant to some extent but again mainly at values below 3,000 $\Omega\,cm^2$. The relationship between the MEPP space constant and membrane resistance is illustrated in Fig. 10*C*. The broken line shows the relationship between the d-c space constant and membrane resistance. The divergence between the d-c space constant and MEPP space constant becomes progressively greater as R_m increases.

Internal Resistivity. The input impedance of a fiber is proportional to the square root of the internal resistivity ($R_i^{\frac{1}{2}}$). It might be expected therefore, that the amplitude of MEPPs would be related to R_i in this way, and this was confirmed.

MEPPs computed for internal resistivities of 350, 250, 150 and 50 Ω cm are shown from above in Fig. 11*A*. The internal resistivity influenced significantly both the amplitude of the voltage response and the effective space constant but had no effect on the time course of MEPPs. In effect, R_i operates as a scaling factor, whether an MEPC or a rectangular current pulse is used as the input. The computed curves (solid lines, Fig. 11*B* and *C*) show the influence of internal resistivity on MEPP amplitude (*B*) and space constant (*C*). The broken line in Fig. 11*C* shows, for comparison, the effect of R_i on the d-c space constant.

Membrane Capacitance. Intuitive arguments, similar to those used to predict the influence of changes in membrane resistance, would suggest that membrane capacitance would have a considerable effect on MEPPs. This was confirmed and the effect is described quantitatively (Fig. 12*A*).

MEPPs computed in fibers with membrane capacitances of 0.5, 2, 6 and 10 $\mu F\,cm^{-2}$ are shown from above down. An increase in membrane capacitance decreases the amplitude and slows the time course of MEPPs. The graph (Fig. 12*B*) shows that the relationship between MEPP amplitude and C_m is steepest as C_m approaches zero. Where $C_m = 0$, the peak height is equal to the voltage response (2 mV) to a rectangular current pulse of the same amplitude as the standard current (5 namps).

Membrane capacitance affects the MEPP space constant also, as illustrated in Fig. 12*C*. As C_m increases, the MEPP space constant becomes shorter. Because the d-c space constant is independent of capacitance the divergence between the d-c space constant (2 mm) and the MEPP space constant becomes greater as C_m increases. Clearly, with the standard cable constants for toad sartorius fibers, membrane capacitance has much more effect than membrane resistance on the amplitude of MEPPs.

Fiber Diameter. Another characteristic of a muscle fiber which has a marked influence on the amplitude of MEPPs is its diameter (Katz & Thes-

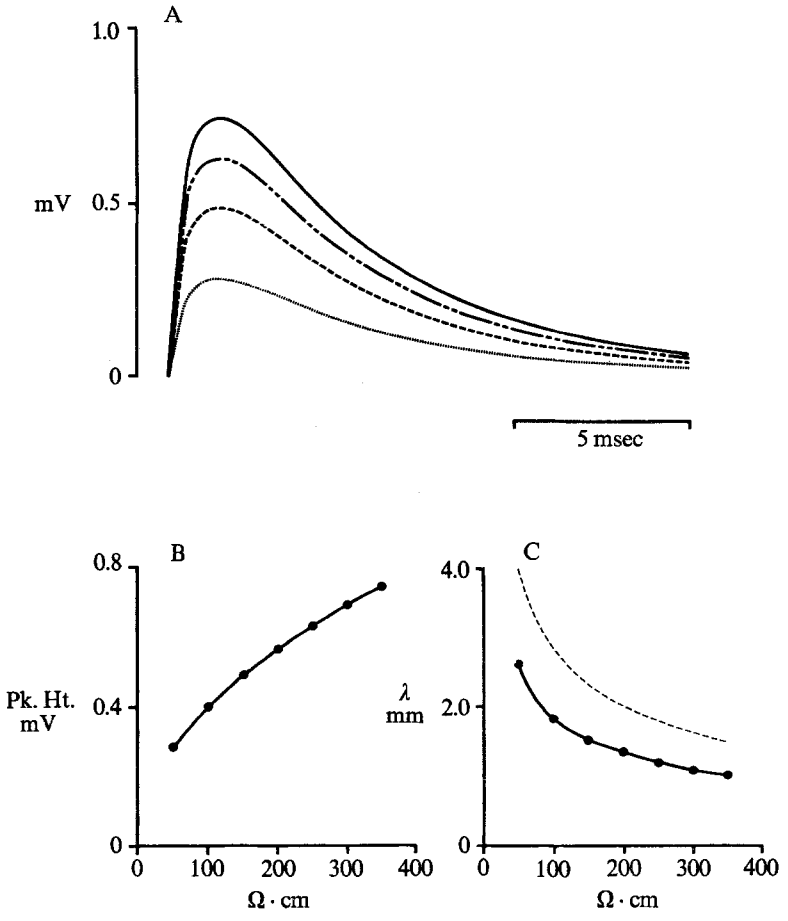

Fig. 11. (*A*) Miniature end plate potentials computed with the standard current and fiber parameters except that the internal resistivity was varied (from above down: 350, 250, 150 and 50 Ω cm). Horizontal calibration, 5 msec. (*B*) Relationship between peak height of the computed voltage responses and internal resistivity. (*C*) Relationship between the space constant of the computed voltage responses and internal resistivity. The broken line shows the relationship with a rectangular current input

leff, 1957). As diameter increases, the amplitude of MEPPs decreases, and this is illustrated in Fig. 13*A* and *B*. MEPPs computed for fiber diameters of 20, 40, 60 and 120 μm are shown from above down in Fig. 13*A*. The computed curve in Fig. 13*B* can be described by the equation $V=410\,d^{-1.5}$, where V is the peak height in mV and d is the fiber diameter in microns. As with R_i, fiber diameter acts as a scaling factor and has no effect on the time course of MEPPs.

Fiber diameter has a parallel effect on the d-c space constant and the MEPP space constant (Fig. 13*C*, broken line and full line, respectively). In both cases, the space constant is related to $d^{\frac{1}{2}}$.

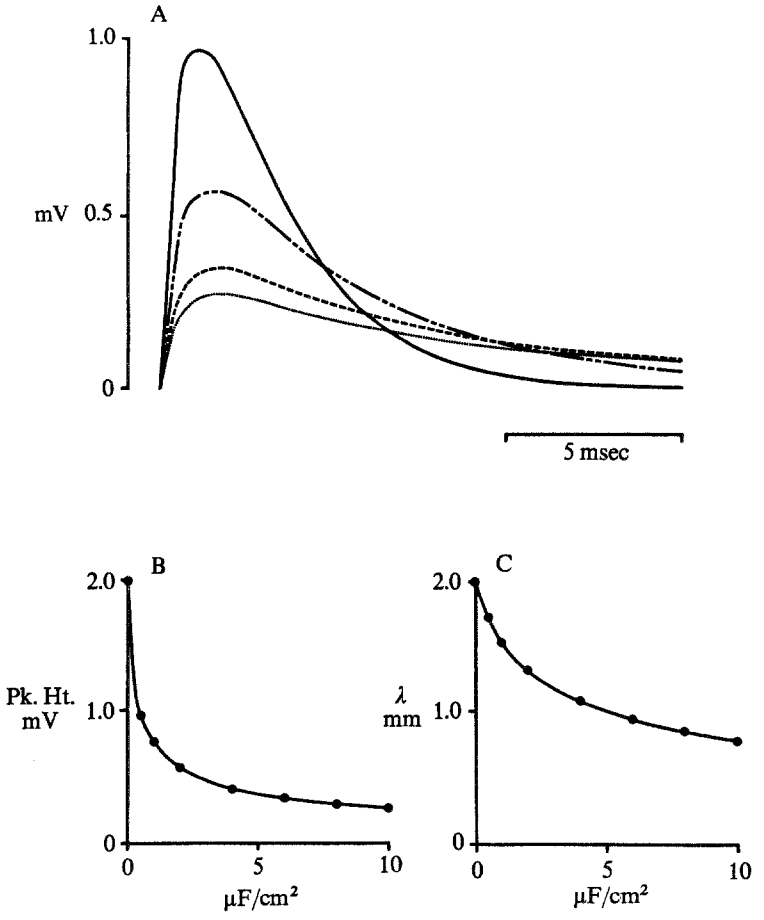

Fig. 12. (*A*) Miniature end plate potentials computed with the standard current input into a standard cable, with variations in the membrane capacitance (from above down: 0.5, 2, 6 and 10 μF cm^{-2}). Horizontal calibration, 5 msec. (*B*) Relationship between peak height of the computed responses and membrane capacitance. (*C*) Relationship between space constant of the peak height of the computed potentials and membrane capacitance

Discussion

The model which was used in this analysis is based on the passive electrical properties of a glycerol-treated muscle fiber. It is possible that the equivalent circuit shown in Fig. 1*B* is not the most accurate description of a glycerol-treated muscle fiber. Hodgkin and Nakajima (1972) have shown that there are two different values of capacitance that can be measured in glycerol-treated muscle fibers. The membrane capacity determined from the conduction velocity and the time constant of the foot of the action

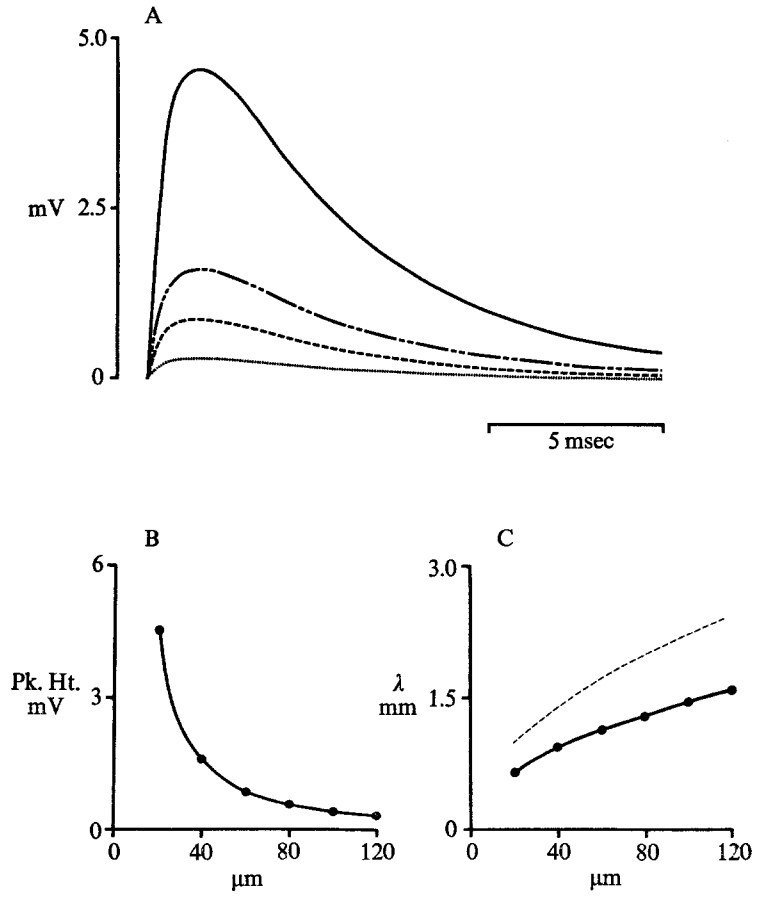

Fig. 13. (*A*) Miniature end plate potentials computed with a standard current input into a standard cable, with variations in fiber diameter (from above down: 20, 40, 60 and 120 μm). Horizontal calibration, 5 msec. (*B*) Relationship between peak height of the computed responses and fiber diameter. (*C*) Relationship between space constant of the peak height of the computed potentials and fiber diameter. The broken line shows the relationship for a rectangular current pulse

potential has a value of 0.9 μF/cm^2, whereas the low frequency capacity is generally about 2 μF/cm^2 (Table 1; Falk & Fatt, 1964; Gage & Eisenberg, 1969; Hodgkin & Nakajima, 1972; Dulhunty & Gage, 1973) and this has led to the suggestion (one of several possible explanations) that 1 μF/cm^2 of the capacity of glycerol-treated fibers comes from residual, intact tubules and is in series with a resistance which isolates it at high frequencies. Even if this is so, and it seems unlikely in view of the electron-microscopic results of Eisenberg and Eisenberg (1968), the full capacitance of 2 μF/cm^2 would be seen at a frequency of 25 Hz (Falk & Fatt, 1964) and the circuit and

equations used here would be appropriate. The argument can be extended further to include a claim for the applicability of these results to normal muscle fibers. Because of the "low frequency" of the voltage response at the origin, the results shown in Fig. 12, in the range 4 to 8 μF/cm^2, probably give a close description of voltage responses to an MEPC in a normal muscle fiber. The increased capacitance would tend to reduce the amplitude of MEPPs and make them decay more slowly. The greater capacitance would make the influence of membrane resistance on the amplitude of MEPPs even less, and would also tend to make the difference between the d-c space constant and MEPP space constant greater than in glycerol-treated fibers (Fig. 12*C*). The presence of a transverse tubular system in normal fibers should not affect the conclusion reached in this investigation, that MEPPs are generated by a local conductance change leading to an MEPC which spreads passively along a fiber. It is remotely possible, perhaps, that there is an active conductance change in the transverse tubular system during MEPPs (or end plate potentials), in which case the hypothesis of passive spread may not hold in normal fibers.

The method of computing voltage responses assumes a uniform (disc) input of current at the middle of an infinite cable whereas an MEPP is probably generated at one point on the surface of a fiber. However, the radius of the fiber is so small compared with the MEPP space constant ($<5\%$) that any difference between a disc and point input of current would be very small.

The spatial distribution of the origins of MEPPs in a fiber (Fig. 3) indicates that the "physiological end plate" extends more than 200 μm along a cell. This confirms previous evidence (Kuhne, 1887; for more recent references, *see* Kuno, Turkanis & Weakly, 1971) of end plates of such length. As MEPPs at any one origin vary in size over a wide range (Fig. 3), the variation in amplitude of MEPPs recorded at one point in a muscle fiber cannot be attributed primarily to a spatial distribution of origins.

The close agreement between computed and observed MEPPs led us to use the model to analyze quantitatively, and in some detail, the effect of the time course of MEPCs, and the properties of the postsynaptic fiber, on MEPPs. Many of the general effects are intuitively obvious. For example, the time constant of the membrane in glycerol-treated muscle fibers is of the order of 8 msec. It is clear that currents which have a duration of less than 8 msec will not "fully charge" the membrane and this is illustrated in Fig. 14. The dotted line in Fig. 14*A* describes rectangular current inputs of 5 namps with different durations (1, 2, 5 and 10 msec; *a*, *b*, *c* and *d*, respectively). The computed voltage responses to these rectangular currents

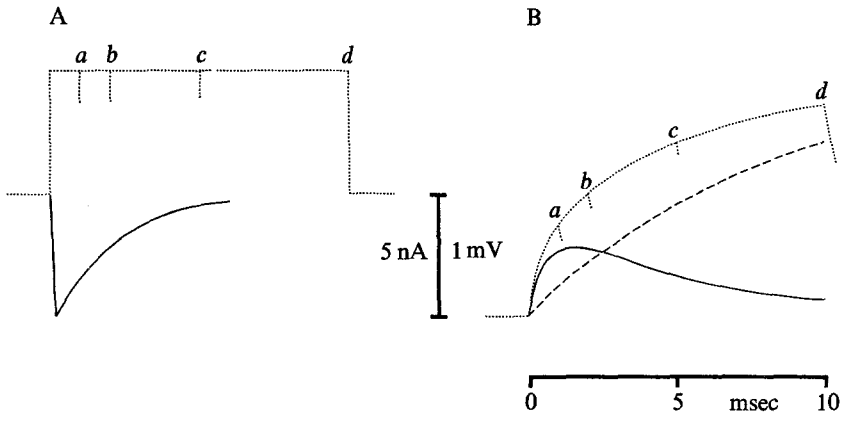

Fig. 14. Computed voltage responses to various current inputs at the origin in a "standard" muscle fiber. (*A*) Input currents. The rectangular current pulses (dotted lines) have the same amplitude but different durations. The downward current represents a miniature end plate current. (*B*) Computed voltage responses to the rectangular current pulses (dotted lines, *a*, *b*, *c* and *d*) and to the miniature end plate current (solid line). The broken line shows an exponential rise of voltage with the time constant ($R_m \cdot C_m$) of the fiber. Vertical calibration: 5 namps, 1 mV

are shown in Fig. 14*B* (dotted lines). For comparative purposes, the standard MEPC is shown in Fig. 14*A* and the computed response in Fig. 14*B*. The voltage responses *a*, *b*, *c* and *d* in Fig. 14*B* follow an error function which is steeper than an exponential with time constant $R_m \cdot C_m$ (broken line, Fig. 14*B*). The responses to the rectangular current pulses could have been predicted using tables of error functions and cable equations. When the input is not a simple function however, the relationship cannot be calculated so simply, but can be computed using the method described in this paper. This allows the relationship between MEPCs and MEPPs, some of which can be predicted qualitatively, to be determined quantitatively.

It is clear that membrane capacitance has a large influence on the voltage response of a toad sartorius fiber to an MEPC, whereas membrane resistance has little effect. On the other hand, Katz and Thesleff (1957) have shown a relationship between input resistance ($\frac{1}{2}\sqrt{r_m r_i}$) and the amplitude of MEPPs in frog sartorius fibers. However, the variation in input resistance from fiber to fiber was probably due to variations in diameter (as inferred by Katz & Thesleff, 1957), not to differences in membrane resistance or internal resistivity, which were presumably similar in each fiber. Input resistance, though not determining the voltage response, is conveniently related to fiber diameter $\left(R_0 = \frac{1}{\pi}\sqrt{R_m R_i}\, d^{-1.5}\right)$ and, as has been shown

(Fig. 10*B*), the amplitude of MEPPs is directly related to $d^{-1.5}$. Using the standard cable properties and standard MEPC (*see* Materials and Methods), the computed constant relating MEPP amplitude to input resistance was found to be 1.42 mV/M Ω, which is rather close to the value of 1.33 mV/M Ω found experimentally in normal fibers (*see* Fig. 5, Katz & Thesleff, 1957). As the peak amplitude of the standard current is 5 namps, this result illustrates again that the effective input impedance of a sartorius fiber "seen" by an MEPC is much less than the input resistance, which would give a relationship of 5 mV/M Ω in our standard fiber.

The concept of a relationship between input resistance and MEPP amplitude may be misleading. If the input resistance of a fiber increases because of an increase in membrane resistance, there may be very little change in the amplitude of MEPPs (Fig. 10*A* and *B*). Conversely, a large change in MEPP amplitude is unlikely to be due to a change in membrane resistance above the normal range of 3,000 to 4,000 Ω cm^2. Of course, in postsynaptic fibers which have a membrane resistance less than 1,000 Ω cm^2 (e.g., muscle fibers in the rat diaphragm), an increase in membrane resistance may well cause an increase in the amplitude of MEPPs.

An increase in the amplitude of a postsynaptic potential, which is not due to an increase in quantal content, has been commonly attributed to an increase in the input resistance of the postsynaptic fiber. It is possible however, that many drugs or procedures which change the amplitude of a synaptic potential postsynaptically, do so by altering the time course of the synaptic current, or by modifying the membrane capacitance of the postsynaptic cell, neither of which would affect the input resistance. An increase in membrane resistance, which would increase input resistance, has little effect on the amplitude of MEPPs (Fig. 10). Again, an increase in membrane resistance would have such little effect, only when the membrane resistance is effectively "shunted" by the membrane capacitance.

Because of the membrane capacitance, the decay time of an MEPC influences the amplitude and time course of MEPPs (Fig. 9). This probably explains the observation of Takeuchi and Takeuchi (1959) that the "effective resistance," given by the ratio of the amplitudes of end plate potentials and end plate currents, is increased when the temperature is lowered. Because the decay time of MEPCs is slowed as the temperature falls (Takeuchi & Takeuchi, 1959; Kordaš, 1972; Magleby & Stevens, 1972; Gage & McBurney, *unpublished observations*) the effective "input impedance" of the muscle fiber might be expected to increase as the temperature falls. Similarly, the amplitude of an end plate potential would be increased by an anticholinesterase which prolongs the end plate current,

(Kordaš, 1972; Magleby & Stevens, 1972; Gage & McBurney, *unpublished observations*), even if the peak amplitude of the end plate current were not increased. It is possible that the input-output function of a synapse could be altered by changes in the time course of synaptic current induced by use or disuse of the synapse. For example, if "conditioning" were to reduce the activity of acetylcholinesterase at a neuromuscular junction, the post-synaptic response to a quantum of transmitter would be increased.

We are indebted to Francesca Stewart, R. Lorenz, J. Fowler and L. Pek for technical assistance and to Drs. P. H. Barry, J. Gras and G. Isaacs for helpful discussion. This work was supported by a grant from the National Health and Medical Research Council of Australia.

References

Carslaw, H. S., Jaeger, J. C. 1963. Operational Methods in Applied Mathematics. Dover Publications Inc., New York.

Dulhunty, A. F., Gage, P. W. 1973. Electrical properties of toad sartorius muscle fibres in summer and winter. *J. Physiol. (In press).*

Eisenberg, B., Eisenberg, R. S. 1968. Selective disruption of the sarcotubular system in frog sartorius muscle. *J. Cell. Biol.* **39**:451.

Eisenberg, R. S., Gage, P. W. 1967. Frog skeletal muscle fibres: Changes in electrical properties after disruption of the transverse tubular system. *Science* **158**:1700.

Eisenberg, R. S., Johnson, E. A. 1970. Three-dimensional electrical field problems in physiology. *Prog. Biophys. Mol. Biol.* **20**:1.

Falk, G., Fatt, P. 1964. Linear electrical properties of striated muscle fibres observed with intracellular electrodes. *Proc. Roy. Soc. (London), B.* **160**:69.

Fatt, P. 1964. An analysis of the transverse electrical impedance of striated muscle. *Proc. Roy. Soc. (London), B.* **159**:606.

Fatt, P., Katz, B. 1951. An analysis of the end-plate potential recorded with an intracellular electrode. *J. Physiol.* **115**:320.

Gage, P. W., Armstrong, C. M. 1968. Miniature end-plate currents in voltage clamped muscle fibres. *Nature* **218**:363.

Gage, P. W., Eisenberg, R. S. 1969. Capacitance of the surface and transverse tubular membrane of frog sartorius muscle fibres. *J. Gen. Physiol.* **53**:265.

Gage, P. W., McBurney, R. N. 1972. Miniature endplate currents and potentials generated by quanta of acetylcholine in glycerol-treated toad sartorius fibres. *J. Physiol.* **226**:79.

Hodgkin, A. L., Nakajima, S. 1972. Analysis of the membrane capacity in frog muscle. *J. Physiol.* **221**:121.

Hodgkin, A. L., Rushton, W. A. H. 1946. The electrical constants of a crustacean nerve fibre. *Proc. Roy. Soc. (London), B.* **133**:444.

Howell, J. N. 1969. A lesion of the transverse tubules of skeletal muscle. *J. Physiol.* **201**:515.

Howell, J. N., Jenden, D. J. 1967. T-tubules of skeletal muscle: Morphological alterations which interrupt excitation-contraction coupling. *Fed. Proc.* **26**:553.

Jack, J. J. B., Redman, S. J. 1971. The propagation of transient potentials in some linear cable structures. *J. Physiol.* **215**:283.

Katz, B. 1948. The electrical properties of the muscle fibre membrane. *Proc. Roy. Soc. (London), B.* **135**:506.

Katz, B., Thesleff, S. 1957. On the factors which determine the amplitude of the "miniature" end-plate potential. *J. Physiol.* **137**:267.

Kordăs, M. 1972. An attempt at an analysis of the factors determining the time course of the end-plate current. *J. Physiol.* **224**:317.

Kuhne, W. 1887. Neue Untersuchungen über motorische Nervenendigung. *Z. Biol.* **23**:1.

Kuno, M., Turkanis, S. A., Weakly, J. N. 1971. Correlation between nerve terminal size and transmitter release at the neuromuscular junction of the frog. *J. Physiol.* **213**:545.

Magleby, K. L., Stevens, C. F. 1972. The effect of voltage on the time course of end-plate currents. *J. Physiol.* **223**:151.

Noble, D., Stein, R. B. 1966. The threshold conditions for initiation of action potentials by excitable cells. *J. Physiol.* **187**:129.

Takeuchi, A., Takeuchi, N. 1959. Active phase of frog's end-plate potential. *J. Neurophysiol.* **22**:395.